



SATELLITE CLUSTERS FOR FUTURE GRAVITY FIELD MISSIONS

Nico Sneeuw and Hanspeter Schaub

**IAG International Symposium
Gravity, Geoid and Space Missions**

Porto, Portugal

Aug. 30 – Sept. 3, 2004

Satellite clusters for future gravity field missions

Nico Sneeuw

Department of Geomatics Engineering, University of Calgary, sneeuw@ucalgary.ca,
currently at: Universität Stuttgart, Geodätisches Institut

Hanspeter Schaub

Aerospace and Ocean Engineering Department, Virginia Tech, schaub@vt.edu

Abstract. The current missions CHAMP and GRACE have already contributed drastically to our knowledge of the Earth's gravity field in terms of accuracy, homogeneity and time- and space-resolution. The future mission GOCE will further add to that in terms of spatial resolution. Nevertheless, each of these missions has its own limitations. At the same time several geoscience disciplines push for ever higher requirements on spatial resolution, time resolution and accuracy. Future gravity field missions will need to address these requirements.

A number of new technologies may enable these future missions. They include laser tracking and atomic interference. Most likely, a mission that implements such technologies, will make use of the concept of formation flying. This paper will discuss the feasibility of low-Earth satellite clusters. It focuses in particular on the stability of satellite formations under the influence of perturbations by the Earth's flattening. Depending on initial conditions several types of relative J_2 orbits can be attained.

2006, aims at cm-accuracy and a spatial resolution corresponding to maximum degree 300. This high resolution, combined with the relatively short mission duration, does not allow time-variable gravity recovery, although time variations will alias into the static solution.

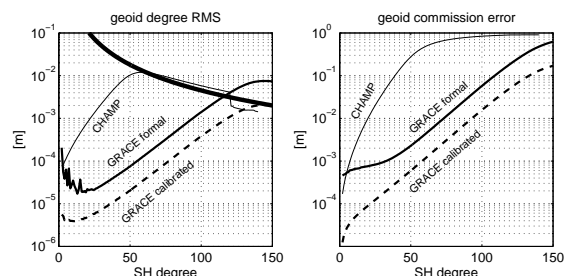


Figure 1. CHAMP and GRACE gravity recovery performance: geoid RMS (left) and cumulative geoid error (right) as function of spherical harmonic degree. The CHAMP curves represent the model EIGEN2. Those of GRACE refer to the model EIGEN-GRACE02S.

1 Limitations of current and planned gravity missions

CHAMP, GRACE and GOCE. The satellite mission CHAMP currently provides static gravity field solutions at dm-level geoid accuracy up to an effective maximum spherical harmonic degree of around 60, cf figure 1. Recovery of the time-variable field seems to be at—or rather below—the edge of feasibility. Although CHAMP is still in orbit, delivering quality science data, this combination of resolution and accuracy is the natural limitation of the mission.

The accuracy of GRACE-derived geoids, on the other hand, is at mm-level around these degrees. It achieves its resolution around degree 120 at which the geoid accuracy is at the dm-level again. Future data and modeling improvements will likely push the limit towards a maximum degree of 150. Moreover, GRACE provides monthly solutions that clearly reveal time-variable gravity (Tapley et al., 2004).

The gradiometer mission GOCE, due for launch in

Despite the wealth of new gravity field information and despite the many new scientific issues that can be addressed, these missions are limited in spatial resolution, temporal behaviour (resolution and mission duration) and accuracy of the resulting gravity field recovery. The key limitations, at least from a gravity recovery viewpoint, are:

- Sampling and resolution: missions are designed for either spatial or spectral resolution. A simultaneous high spatial and spectral resolution is fundamentally impossible with a single mission.
- Aliasing: phenomena with sub-monthly period will alias into the monthly GRACE solutions. Time-variable signal will also map into the static GOCE field.
- Monitoring: limited mission durations of 5 year (CHAMP, GRACE) or 1 year (GOCE).
- Gravity signal: the GRACE-observable is a relatively weak observable, see below.

The limitations of GRACE and GOCE are analyzed from a more technological viewpoint by Aguirre-Martinez and Sneeuw (2003).

Future low-low SST. At the same time Earth scientists are driving the requirements for ever higher accuracies and resolutions. Moreover, similar to satellite radar altimetry, there is a growing demand for a monitoring facility rather than a few individual satellite missions. Studies into next-generation gravity field missions tend to focus on low-low satellite-to-satellite tracking (SST). Indeed, the accuracy gain that is potentially achieved by laser SST over a GRACE-type radio link is far larger than the expected future improvements in gradiometry technologies.

The key GRACE-type SST observable is the inter-satellite distance and relative velocity in a leader-follower configuration at near-polar inclination. This type of observable inherently suffers from the weakness that it is mainly sensitive along the line-of-sight, i.e. in North-South direction. This was demonstrated by the very first release of a GRACE map, cf. Figure 2, which clearly demonstrated a sensitivity towards East-West features in the Earth's gravity field. Note, for instance, the weak presence of Andes or Rocky Mountains in the map.

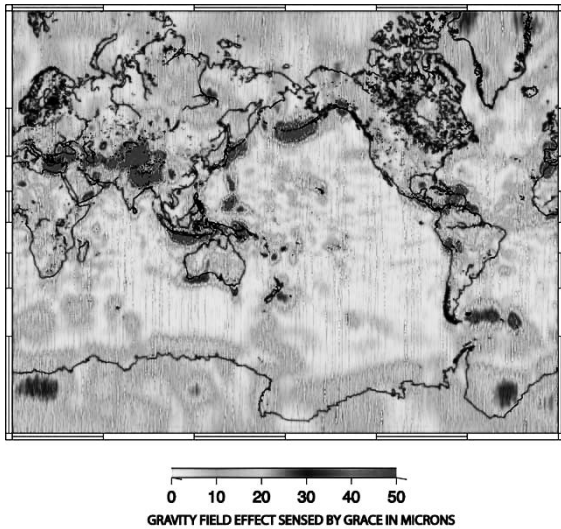


Figure 2. GRACE *first light*: map of gravity field effect on inter-satellite baseline.

The observable approximates the along-track gravity gradient term V_{xx} . This is a relatively weak term. Its spectral content is approximately one half of the radial gravity gradient term V_{zz} . More importantly, the directional sensitivity of the observable also translates into a non-isotropic error behaviour.

Formation flying. Formation flying, which is currently receiving much attention internationally, may solve some of the aforementioned issues. A satellite formation may consist of any number of satellites that are performing a relative motion around a common center. A GRACE-type leader-follower formation is a trivial example. Satellites may also perform elliptical or circular relative motion. Obviously, when the distances between these satellites would be measured, the gravitational signal would include radial information. Moreover, a relative inclination might be achieved that would lead to cross-track information going into the observable. Such observables could address several of the aforementioned weaknesses, most notably the spectral content and the non-isotropy of the low-low SST observable. Including cross-track information may also reduce the aliasing problem.

For these reasons this paper will mainly investigate the feasibility of formation flying in a realistic gravity field. It will then be discussed how to use formation flying in a gravity field mission.

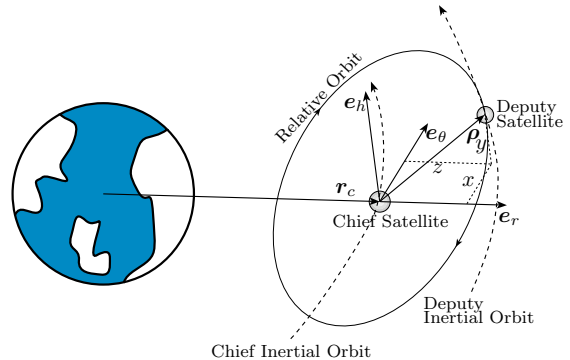


Figure 3. Illustration of a general spacecraft formation with out-of-plane relative motion.

2 Feasibility of formation flying in a J_2 gravity field

2.1 Equations of relative motion

Let us adopt the following formation flying notation. A set of deputy satellites are to fly about a chief location as shown in Figure 3. This location could be an actual spacecraft, or simply a reference point. The inertial chief position vector is r_c , while ρ is the deputy relative position vector. The rotating Hill frame $\mathcal{O} = \{e_\theta, e_h, e_r\}$ is defined with e_r being along the chief orbit radial, e_h being along the chief orbit plane normal, and e_θ completing the right handed coordinate system. The angular rate of the

Hill frame (chief motion) is $\dot{\theta}$. The deputy position vector ρ is then expressed in the Hill frame through

$${}^{\mathcal{O}}\rho = (x, y, z)^T \quad (1)$$

The general linearized equations of motion of a deputy satellite with respect to a chief is given by Schaub and Junkins (2003):

$$\ddot{x} + z\ddot{\theta} + 2\dot{z}\dot{\theta} - x\left(\dot{\theta}^2 - \frac{\mu}{r_c^3}\right) = a_x \quad (2a)$$

$$\ddot{y} + \frac{\mu}{r_c^3}y = a_y \quad (2b)$$

$$\ddot{z} - z\left(\dot{\theta}^2 + 2\frac{\mu}{r_c^3}\right) - x\ddot{\theta} - 2\dot{x}\dot{\theta} = a_z \quad (2c)$$

where μ is the gravitational constant and (a_x, a_y, a_z) are non-Keplerian forces acting on the deputy satellite. They could be due to atmospheric drag, J_2 gravitational oblateness effects, or control thrusters.

Many missions consider formations where the chief motion is essentially circular with a near zero eccentricity e . In this case the chief rate $\dot{\theta}$ is constant and equal to the mean orbit rate $n = \sqrt{\mu/r_c^3}$. The equations of motion simplify to the well-known Clohessy-Wiltshire (CW) equations (Clohessy and Wiltshire, 1960):

$$\ddot{x} + 2n\dot{z} = a_x \quad (3a)$$

$$\ddot{y} + n^2y = a_y \quad (3b)$$

$$\ddot{z} - 2n\dot{x} - 3n^2z = a_z \quad (3c)$$

These equations are sometimes also referred to as Hill's equations. Eq. (3) has been used extensively in spacecraft formation flying mission analysis and control research. They are reasonable as long as (x, y, z) are small compared to the chief orbit radius r_c . Instead of using rectilinear local coordinates (x, y, z) , the relative motion can also be expressed through the curvilinear coordinates $(\delta\theta, y, \delta r)$, (Schaub and Junkins, 2003):

$$r_c\delta\ddot{\theta} + 2n\delta\dot{r} = a_x \quad (4a)$$

$$\ddot{y} + n^2y = a_y \quad (4b)$$

$$\delta\ddot{r} - 2nr_c\delta\dot{\theta} - 3n^2\delta r = a_z \quad (4c)$$

Note that Eqs. (4) are algebraically equivalent to the CW equations, but provide greatly improved modeling accuracy. This is achieved by interpreting the relative motion coordinates differently. The z coordinate is now interpreted as a difference in orbit radii, while the x coordinate is interpreted as difference in argument of latitude θ . Such cylindrical coordinates

will closely match the relative motion for near circular chief motion. Along track motions have the natural bending that leader-follower formations would exhibit.

Often it is convenient to work in non-dimensional states. Let $(u, v, w) = (x, y, z)/r_c$ be non-dimensional deputy relative position coordinates. If the true anomaly f is used as the independent angle instead of time, then the general first order equations of motion are given through:

$$u'' + 2w' = \alpha_u \quad (5a)$$

$$v'' + v = \alpha_v \quad (5b)$$

$$w'' - 2vv' - \frac{3w}{1 + e \cos f} = \alpha_w \quad (5c)$$

Many further forms of the relative motion have been developed. Schweighart and Sedwick (2002) developed an extension to the CW equations which includes linear J_2 oblateness perturbations in the equations of motion. Humi and Carter (2003) have shown solutions with special forms of quadratic drag. An excellent survey of relative motion state transition matrices is found in (Carter, 1998).

2.2 First order analytical solutions

If the chief motion can be modeled as circular, then the CW equations can be solved analytically. Assuming no perturbations or thrusting is present ($a_x = a_y = a_z = 0$), all possible deputy relative motions can be expressed in closed form (Schaub and Junkins, 2003):

$$x(t) = -2A_0 \sin(nt + \alpha) - \frac{3}{2}ntz_{\text{off}} + x_{\text{off}} \quad (6a)$$

$$y(t) = B_0 \cos(nt + \beta) \quad (6b)$$

$$z(t) = A_0 \cos(nt + \alpha) + z_{\text{off}} \quad (6c)$$

Note that the out-of-plane motion is decoupled from the in-plane motion. The integration constants can be expressed in terms of initial conditions through:

$$A_0 = \frac{1}{n} \sqrt{\dot{z}_0^2 + (2\dot{x}_0 + 3nz_0)^2} \quad (7a)$$

$$B_0 = \frac{1}{n} \sqrt{\dot{y}_0^2 + (ny_0)^2} \quad (7b)$$

$$\alpha = \arctan\left(\frac{-\dot{z}_0}{-(3nz_0 + 2\dot{x}_0)}\right) \quad (7c)$$

$$\beta = \arctan\left(\frac{-\dot{y}_0}{ny_0}\right) \quad (7d)$$

$$z_{\text{off}} = \frac{2}{n} (\dot{x}_0 + 2nz_0) \quad (7e)$$

$$x_{\text{off}} = x_0 - \frac{2\dot{z}_0}{n} \quad (7f)$$

These equations are very convenient to explore what possible *natural* and unforced formation shapes are feasible. For example:

- If $B_0 = 0$, a purely in-plane relative motion is achieved which is always a 2:1 ellipse (the CartWheel-mode);
- If $B_0 = \sqrt{3}A_0$, the relative motion is circular with radius $2A_0$ (the LISA-mode);
- If $B_0 = 2A_0$, one achieves elliptical motion with a circular cross-section in the local horizon plane $e_\theta - e_h$ (the TechSat21-mode).

The latter two configurations also require either $\alpha = \beta$ or $\alpha = \beta + \pi$.

If the chief motion is not circular, then the solution in Eq. (6) is no longer valid. Even small amounts of eccentricity can produce modeling errors comparable to those produced by J_2 gravitational perturbations or atmospheric drag. Carter (1998) presents an analytical solution to the linearized relative motion where the true anomaly is used as the independent variable. However, this solution does not provide that elegant geometrical insight the classical CW solution provides. In (Schaub, 2004) the first order (u, v, w) non-dimensional relative motion is expressed in terms of orbit element differences. This analytical relative motion solution is valid for chief motions of any eccentricity, but also uses true anomaly as the independent variable. The orbit element difference based solution is written in terms of static offsets and sinusoidal components, and has a similar geometric structure as the analytical CW solution. Even for highly eccentric chief motions, the first order out-of-plane relative motion is still decoupled from the in-plane motion.

2.3 Bounded relative motion constraints

To avoid having the formation drift apart, bounded relative motion solutions are sought. If no perturbations are present, then the nonlinear bounded relative motion constraint is simply that all orbit periods must be equal. This is equivalent to requiring that the semi-major axis differences δa be zero. This bounded motion constraint is valid for both circular and eccentric orbits, as well as small and large relative orbit dimensions.

The orbit element constraint $\delta a = 0$ can be approximated using Hill frame Cartesian coordinates by taking a first order expansion. An equivalent approach is to look at the analytical CW solution in Eq. (6). The only secular growth occurs in the along track direction through the $-3/2ntz_{\text{off}}$ term. For this

secular growth term to be zero, we find that the initial Cartesian coordinate conditions must satisfy

$$\dot{x}_0 + 2nz_0 = 0 \quad (8)$$

This first order approximation of $\delta a = 0$ assumes that the chief is circular and that the relative orbit radius ρ is small compared to the chief orbit radius r_c . However, this condition can be applied at any point within the orbit. If the chief motion has a small but non-zero eccentricity, then the first order bounded relative motion constraint is written as (Schaub and Junkins, 2003; Inalhan et al., 2002):

$$\dot{x}_0(2 + 3e)z_0 = 0 \quad (9)$$

if the initial time is set at perigee. If t_0 is set at apogee, then the constraint is (Schaub and Junkins, 2003):

$$\dot{x}_0(2 - 3e)z_0 = 0 \quad (10)$$

These conditions are not valid at any other orbit point.

If the gravitational J_2 perturbation is present, then all orbits experience short and long period perturbations. Only the ascending node Ω , argument of perapsis ω and initial mean anomaly M_0 will experience secular drift. Their mean rates are given by (Schaub, 2004; Schaub and Alfriend, 2001):

$$\frac{d\Omega}{dt} = -\frac{\epsilon(a, e)}{2}n \cos i \quad (11a)$$

$$\frac{d\omega}{dt} = \frac{\epsilon(a, e)}{4}n (5 \cos^2 i - 1) \quad (11b)$$

$$\frac{dM_0}{dt} = \frac{\epsilon(a, e)}{4}n \eta (3 \cos^2 i - 1) \quad (11c)$$

with $\epsilon(a, e) = 3J_2(r_{\text{eq}}/a(1 - e^2))^2$ and where $\eta = \sqrt{1 - e^2}$ is an eccentricity measure. The distance r_{eq} is Earth's equatorial radius. Note that only a , e and i control the secular drift rate of the remaining three orbit elements. This drift could be compensated for by thrusting. However, this will quickly consume a lot of fuel. Schaub and Alfriend (2001) introduce the concept of J_2 -invariant relative orbits. Here the relative orbit geometry is designed such that while all orbits are still drifting, on average, they will drift at equal rates. To achieve this, the following mean relative drift rates are set to zero:

$$\delta\dot{\theta} = \delta\dot{\omega} + \delta\dot{M}_0 = 0 \quad (12)$$

$$\delta\dot{\Omega} = 0 \quad (13)$$

The first condition guarantees no in-plane drift and leads to the orbit element constraint equation

$$\frac{\delta a}{a} = \frac{J_2}{2} \frac{a^2}{r_{\text{eq}}^2} \frac{1}{\eta} (4 + 3\eta)(1 + 5 \cos^2 i) \delta \eta \quad (14)$$

The second conditions controls the out-of-plane drift. It yields the orbit element constraint

$$\delta \eta = -\frac{\eta}{4} \tan i \delta i \quad (15)$$

By choosing either a difference in eccentricity, inclination, or semi-major axis, the other two orbit element differences are then dictated through the constraints in Eqs. (14) and (15). Note that in order to have either a difference in eccentricity or inclination, a non-zero difference in semi-major axis is required. This is a departure from the Keplerian bounded relative motion results. For near-polar chief motions, the J_2 -invariance constraints result in very large along track relative orbit dimensions. To avoid this, the 2nd constraint in Eq. (15) is typically dropped and any out-of-plane secular drift will have to be compensated for through thrusting (Schaub and Junkins, 2003). When designing J_2 -invariant relative orbits, the motion is typically described in mean element space, cf. (Schaub and Alfriend, 2001; Brouwer, 1959). To map between the osculating (instantaneous) orbit elements and the mean orbit elements (long period and secular terms removed), the Brouwer-Lyddane theory can be used (Lyddane, 1963; Brouwer, 1959).

3 Gravity mapping from satellite formations

Future low-low sst missions, whether formation flying or not, will most likely employ laser technology for the intersatellite link. Bender et al. (2003) discuss heterodyne laser interferometry, whereas McGuirk et al. (2002) discuss atomic interference. Differential accelerometry seems feasible at a level of $10^{-12} \text{ m s}^{-2}/\sqrt{\text{Hz}}$. Over a baseline of 1 km this would translate already into gradiometry at the $10^{-6} \text{ E}/\sqrt{\text{Hz}}$ level. The baseline length immediately scales into the error level.

The range rate $\dot{\rho}$ between two satellites is the projection of the relative vectorial velocity $\dot{\boldsymbol{\rho}}$ on the line-of-sight unit vector \mathbf{e} , e.g. (Rummel et al., 1978):

$$\dot{\rho} = \dot{\boldsymbol{\rho}} \cdot \mathbf{e} \quad (16a)$$

$$\Rightarrow \ddot{\rho} = \ddot{\boldsymbol{\rho}} \cdot \mathbf{e} + \frac{1}{\rho} (\dot{\boldsymbol{\rho}} \cdot \dot{\boldsymbol{\rho}} - \dot{\rho}^2) \quad (16b)$$

Using Newton's equations, the vectorial acceleration difference $\ddot{\boldsymbol{\rho}}$ equals the difference in gravitational at-

traction ∇V between the forces. The scalar range acceleration $\ddot{\rho}$ can be obtained from the observed range rate by numerical differentiation. To extract the gravitational information, one should further correct for the relative velocity terms at the right of (16b).

Gradiometry from satellite formations. Alternatively, when dividing $\dot{\boldsymbol{\rho}} \cdot \mathbf{e}$ by the baseline, one obtains the in-line gravity gradient in the baseline direction $\mathbf{e} \mathbf{V} \mathbf{e}$, with \mathbf{V} the gravity gradient tensor. With the baseline close to along-track direction, this observable is mainly V_{xx} . Again, one should correct for the relative velocity terms at the right hand side of (16b). Moreover, one has to account for a linearization error in the approximation $V_{xx} \approx (V_{x,2} - V_{x,1})/(x_2 - x_1)$.

In a satellite formation, the baseline performs a full revolution in the Hill frame \mathcal{O} , i.e. the direction \mathbf{e} rotates once every orbital revolution. Thus the observed gravity gradient $\mathbf{e} \mathbf{V} \mathbf{e}$ contains projections of several tensor components V_{ij} , $i, j \in \{x, y, z\}$. The gravity gradient tensor \mathbf{V} transforms under a rotation of the coordinate frame as $R \mathbf{V} R^T$, in which R denotes the rotation matrix. Let us consider one satellite pair only in the simplest formation, namely the 2:1-ellipse in the orbital plane. Now assume a time-variable rotation α about the y -axis, such that the two satellites are always on the new x' -axis. The coplanar gradients V_{xx}, V_{xz}, V_{zz} project onto the observable as follows:

$$V_{x'x'} = \cos^2 \alpha V_{xx} + 2 \cos \alpha \sin \alpha V_{xz} + \sin^2 \alpha V_{zz}$$

The observable $V_{x'x'}$ ($= \mathbf{e} \mathbf{V} \mathbf{e}$) contains the required gravity observable already. However, if one wants to disentangle the 3 contributing tensor components in the Hill frame, 3 independent intersatellite distances need to be tracked. With 3 different angles α one would have 3 simultaneous equations of the above kind, leading to an instantaneous determination of V_{xx}, V_{xz} and V_{zz} . This can either be realized by a CartWheel of 3 satellites, measuring in a triangle, or by 6 satellites, measuring along the spokes of the wheel, cf. figure 4. The spokes configuration may be easier to realize at the cost of more satellites. The intersatellite links in the triangular formation are dependent. Technologically that may be more demanding, but it has the added benefit that the required orientations are better constrained.

Gradiometry of out-of-plane components (V_{xy}, V_{yy}, V_{yz}) can only be achieved through non-coplanar satellite configurations. A relative inclination of the formation w.r.t. the orbit plane can be represented by a rotation $R_x(\beta)$. Along the same



Figure 4. Potential coplanar configurations for measuring the in-plane V_{xx} , V_{xz} and V_{zz} simultaneously: triangle edges (left) or spokes (right).

lines of arguing as above it can be demonstrated that all gravity gradient tensor components will generally project onto a particular $V_{x'x'}$. To disentangle this projection, 6 instantaneous intersatellite distances should be measured. Thus formation flying offers a way of full-tensor gravity gradiometry.

4 Conclusion

When designing future gravity field missions, formation flying is a viable alternative to leader-follower low-low SST configurations. Despite the presence of perturbations—the strongest being the Earth’s oblateness—stable configurations exist. The homogeneous Clohessy-Wiltshire equations (Hill equations) demonstrate which natural formation shapes are possible. In its simplest form, a 2:1 relative ellipse, the radial gravity gradient V_{zz} is projected onto the SST observable. Thus, the inherent weakness and the non-isotropic behaviour of the conventional low-low SST observable can be solved by formation flying.

Gravity field recovery can be based on observed range rates $\dot{\rho}$. Alternatively they may be differentiated numerically into $\ddot{\rho}$, which can be interpreted as differences in the gravitational attraction between the satellites. Moreover, $\ddot{\rho}$ can be recast into a gravity gradient observable eVe . With sufficiently many satellites linked together in a strategic way, one can even achieve full-tensor gravity gradiometry.

If the relative orbits comprise a cross-track motion, the corresponding observables gain sensitivity in East-West direction. Although this may be helpful in dealiasing signals, the fundamental temporal-spatial sampling problem of a gravity field satellite mission is not addressed. To overcome aliasing multiple-formation configurations must be considered, such as the planned geomagnetic field mission SWARM: one satellite pair at the same altitude but with different right-ascension, plus a single higher satellite.

Finally, if the individual satellites can be designed and launched in a cost-effective way, a formation flying mission would be suitable as a long-term moni-

toring mission.

Acknowledgments. Nico Sneeuw acknowledges the support of the Alexander von Humboldt Foundation and of the GEOIDE Network of Centres of Excellence.

References

- Aguirre-Martinez, M. and Sneeuw, N. (2003). Needs and tools for future gravity measuring missions. *Space Science Reviews*, 108(1-2):409–416.
- Bender, P. L., Hall, J. L., Ye, J., and Klipstein, W. M. (2003). Satellite-satellite laser links for future gravity missions. *Space Science Reviews*, 108(1-2):377–384.
- Brouwer, D. (1959). Solution of the problem of artificial satellite theory without drag. *The Astronomical Journal*, 64(1274):378–397.
- Carter, T. E. (1998). State transition matrix for terminal rendezvous studies: Brief survey and new example. *Journal of Guidance, Control and Dynamics*, 31(1):148–155.
- Clohessy, W. H. and Wiltshire, R. S. (1960). Terminal guidance system for satellite rendezvous. *Journal of the Aerospace Sciences*, 27(9):653–658.
- Humi, M. and Carter, T. (2003). The Clohessy-Wiltshire equations can be modified to include quadratic drag. In *Proc. AAS/AIAA Space Flight Mechanics Meeting*, number AAS 03–240, Ponce, Puerto Rico. AAS/AIAA.
- Inalhan, G., Tillerson, M., and How, J. P. (2002). Relative dynamics & control of spacecraft formations in eccentric orbits. *Journal of Guidance, Control and Dynamics*, 25(1):48–59.
- Lyddane, R. H. (1963). Small eccentricities or inclinations in the Brouwer theory of the artificial satellite. *The Astronomical Journal*, 68(8):555–558.
- McGuirk, J. M., Foster, G. T., Fixler, J. B., Snadden, M. J., and Kasevich, M. A. (2002). Sensitive absolute-gravity gradiometry using atom interferometry. *Physical Review A*, 65:doi 10.1103/PhysRevA.65.033608.
- Rummel, R., Reigber, Ch., and Ilk, K.-H. (1978). The use of satellite-to-satellite tracking for gravity parameter recovery. In *Proc. European Workshop On Space Oceanography, Navigation And Geodynamics (SONG)*, volume SP-137, pages 153–161, Schloss Elmau. ESA.
- Schaub, H. (2004). Relative orbit geometry through classical orbit element differences. *Journal of Guidance, Control and Dynamics*, accepted.
- Schaub, H. and Alfriend, K. T. (2001). J_2 invariant relative orbits for spacecraft formations. *Celestial Mechanics and Dynamical Astronomy*, 79(2):77–95.
- Schaub, H. and Junkins, J. L. (2003). *Analytical Mechanics of Space Systems*. AIAA Education Series, Reston, VA.
- Schweighart, S. A. and Sedwick, R. J. (2002). A high fidelity linearized J_2 model for satellite formation flight. *Journal of Guidance, Control, and Dynamics*, 6(25):1073–1080.
- Tapley, B. D., Bettadpur, S., Ries, J. C., Thompson, P. F., and Watkins, M. M. (2004). GRACE measurement of mass variability in the Earth system. *Science*, 305:503–505.